# Advanced Synthesis & Catalysis

## Accepted Article

**Title:** Catalytic Hydrogenation of CO2 to Formic Acid in DMSO-based Reaction Media: Solved and Unsolved Challenges for Process Development

**Authors:** Christian Jens, Martin Scott, Bastian Liebergesell, Christian Westhues, Pascal Schäfer, Giancarlo Franciò, Kai Leonhard, Walter Leitner, and André Bardow

# Rh-Catalyzed Hydrogenation of $CO_2$ to Formic Acid in DMSO-based Reaction Media: Solved and Unsolved Challenges for Process Development

Christian M. Jens,[a#] Martin Scott,[b#] Bastian Liebergesell,[a] Christian G. Westhues,[b] Pascal Schäfer,[a] Giancarlo Franciò,[b] Kai Leonhard,[a] Walter Leitner[b,c]* and André Bardow[a]*

[a]  Chair of Technical Thermodynamics, RWTH Aachen University, Schinkelstrasse 8, 52062 Aachen, Germany
     [Tel.: +49 241 80 95380; Fax: +49 241 80 92255; andre.bardow@ltt.rwth-aachen.de]
[b]  Institut für Technische und Makromolekulare Chemie, RWTH Aachen University, Worringerweg 2, Aachen, 52074, Germany
[c]  Max Planck Institute for Chemical Energy Conversion, Stiftstr. 34 – 36, Mülheim an der Ruhr, 45470, Germany
     [Tel.: +49 208 306 3614; Fax: +49 208 306 3951; leitner@cec.mpg.de]

**Abstract.** Process concepts have been conceived and evaluated for the amine-free homogeneous catalyzed hydrogenation of $CO_2$ to formic acid (FA). Base-free DMSO-mediated production of FA has been shown to avoid the formation of stable intermediates and thus the energy-intensive FA recovery strategies. Here, we address the challenges in the development of an overall process: from catalyst immobilization to the FA isolation. The immobilization of the homogeneous catalyst was achieved using a multiphase approach (*n*-heptane/DMSO) ensuring high retention of the catalyst (>99%) and allowing facile separation of the catalyst-free product phase. We show that the strong molecular interactions between DMSO and FA on the one hand shift the equilibrium towards the product side,

on the other hand, lead to the formation of an azeotrope preventing a simple isolation step by distillation. Thus, we devised an isolation strategy based on the use of co-solvents and computed the energy demands. Acetic acid was identified as best co-solvent and its compatibility with the catalyst system was experimentally verified. Overall, the outlined process involving DMSO and acetic acid as co-solvent has a computed energy demand on a par with state-of-the-art amine-based processes. However, the insufficient chemical stability of DMSO poses major limitations on processes based on this solvent.

**Keywords:** Carbon Dioxide Hydrogenation; Biphasic Catalysis; PC-SAFT; COSMO-RS; DMSO decomposition

## Introduction

Formic acid (FA, HCOOH) is a commodity chemical product with a variety of agricultural and industrial applications.[1] The annual production amounts to 697 kt (2013)[2] with main uses for silage, in animal feed fermentation, and food preservation, for leather and textile treatment as well as in the chemical, rubber and steel industry.[1b] These markets are strongly influenced by the growth of the population and the demand of FA is thus expected to rise. FA is produced in a two-step process from carbon monoxide as carbon source, which is typically obtained from fossil resources. The use of waste carbon dioxide as starting material for FA production would be a step towards a more sustainable chemical production reducing the environmental impact in terms of carbon footprint and fossil resource depletion.[2a, 3] The competitiveness of such a process is maximized when $CO_2$ is harvested at point

sources like power plants, fermentation and biogas facilities, or steel industry.[4] Additionally, FA could be used as chemical storage of hydrogen originating from surplus renewable energy, thereby facilitating the transition from fossil to a circular energy economy.[1b, 5] Thus, the reversible hydrogenation/dehydrogenation of $CO_2$ is a widely discussed option for interfacing the energy with the chemical sector.[6] Compared to other storage materials,[5a, 7] FA has a relatively low mass fraction of hydrogen (4.4 wt%). However, this drawback might be offset as FA can be directly used in certain applications, *e.g.* in form of FA fuel cells (DFAFCs).[7-8] Furthermore, FA has been suggested as a practical carbon monoxide surrogate and stable formal intermediate of the reverse water gas shift reaction (rWGS).[8-9] Latest research has shown that the decarbonylation/dehydration of FA can be carried out with a wide range of commercially available catalysts such as transition metal doted zeolites.[10] While the use of FA as CO storage system has

1

received less attention up to now, the mass fraction of 60.8 wt% makes FA attractive as a liquid CO-source that can be readily transported and distributed.[11]
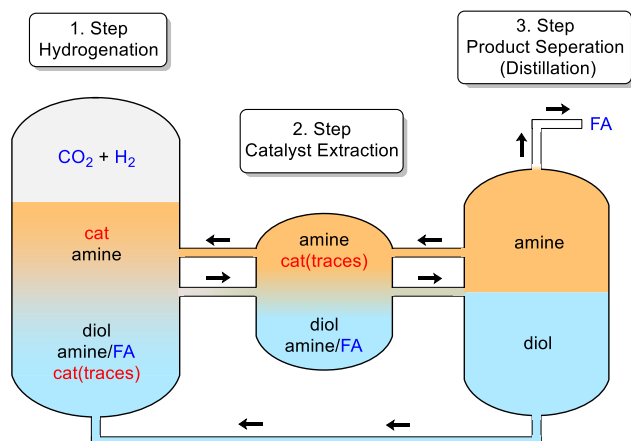


**Figure 1.** BASF process for the hydrogenation of $CO_2$ to FA using $NHex_3$ and a biphasic system.

Among the concepts for integrated hydrogenation and FA isolation, the process developed by BASF was studied in detailed and operated at a mini plant scale (Figure 1).[12] It is thus used as benchmark for the analysis in the present paper. This process uses an apolar amine ($NHex_3$) as stabilizing agent forming an adduct with FA and as catalyst phase at the same time, whereas a polar diol is used as the product phase. Because of some catalyst leaching in the product phase, an additional extraction with $NHex_3$ is necessary before the product mixture can be subjected to thermal cleavage of the FA-$NHex_3$ adduct and FA distillation. Most recently, it has also been demonstrated that aqueous amine solutions, as used for $CO_2$ scrubbing from flue gases, can directly be hydrogenated in a biphasic system with excellent catalyst retention and recyclability leading to the attractive prospect of an integrated $CO_2$-capture and utilization process.[13] Nonetheless, the separation step(s) and isolation of pure FA from amine-based processes are complex and energy demanding motivating the search for alternative solutions.[2a]

Sufficient stabilization to shift the equilibrium towards FA can also be provided by a suitable solvent avoiding the use of an amine. For instance, water stabilizes FA thanks to the hydrogen bonding,[14] resulting in a major enthalpic contribution from solute-solvent interaction. At the same time, solvation of the reactive gases lowers the entropic penalty in the Gibbs free energy of the transformation. Similarly, hydrogen bonds between FA and dipolar aprotic solvents such as dimethyl sulfoxide (DMSO) are particularly effective in stabilizing FA.[15] Recently, Moret, Dyson, and Laurenczy reported the hydrogenation of $CO_2$ in DMSO under relatively mild conditions obtaining FA concentrations up to the range of 2 M, the highest FA concentration for base-free systems currently known.[16] For the solvation process, the thermodynamic boundaries were

determined experimentally and the effect of hydrogen bonding was analyzed in detail by DFT calculations.[15c, 17]

It might be expected that the reduced number of components of the binary FA/solvent mixture as compared to the ternary FA/base/solvent mixture could simplify the downstream processing of the catalytic $CO_2$ hydrogenation in DMSO. However, no overall process schemes and no experimental or process simulation data for solvent-using processes are currently available to corroborate this assumption.
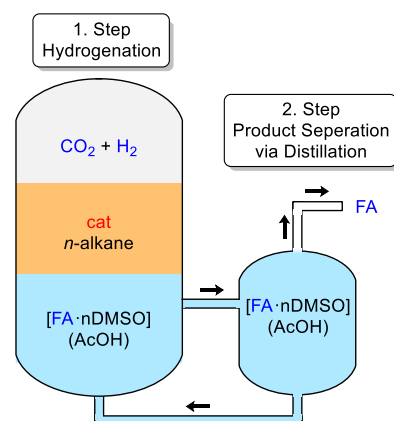


**Figure 2.** Base-free process designed in this work using a biphasic system (*n*-heptane/DMSO) and a co-solvent (AcOH).

Herein, we present the first detailed process design for a base-free FA synthesis based on DMSO as a stabilizing solvent (Figure 2). The hydrogenation of $CO_2$ to FA has been carried out in a biphasic system *n*-heptane/DMSO using Rh-catalysts with tailored apolar phosphine ligands. Facile separation of a catalyst-free product phase suitable for FA isolation and catalyst reutilization has been demonstrated. For the downstream processing, DMSO is shown to form an azeotrope with FA. To overcome the DMSO-FA azeotrope, the use of a co-solvent was found to be key for isolation of FA via a single column distillation. The use of an in silico solvent selection procedure via the quantum-mechanics-based thermodynamic model COSMO-RS allowed the identification of acetic acid as suitable co-solvent. The tolerance of acetic acid in the hydrogenation step was experimentally verified and useful FA concentrations have been achieved. The detailed analysis of the devised process scheme predicts an energy demand comparable with benchmark amine-based processes.[12, 18] However, the insufficient chemical stability of DMSO during the FA isolation step has been recognized as major limitation.

## Results and Discussion

### Hydrogenation of $CO_2$ to FA in a DMSO/*n*-alkane biphasic system

2

The hydrogenation of $CO_2$ to FA in DMSO is an equilibrium reaction (Scheme 1). Catalysts promoting the conversion of $CO_2$ to FA under hydrogen pressure are usually capable to catalyze the back reaction, i.e. the decomposition of FA to hydrogen and carbon dioxide, once the overpressure is released and moderate temperature are applied.[19]

$$H_2 \; + \; CO_2 \; + \; O{=}S\diagup \quad \underset{p\leq 1 \text{ bar, } \Delta T}{\overset{[cat]}{\rightleftharpoons}} \quad HCOOH_{DMSO\ solv}$$
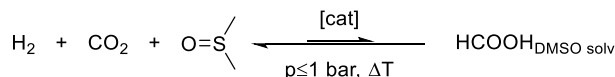
**Scheme 1.** Hydrogenation of carbon dioxide in DMSO.

For instance, when the Wilkinson catalyst [Rh(PPh_3)_3Cl] is added to a 1.4 M solution of FA in DMSO, the FA concentration decreases to 0.7 M within 16 h at a temperature of 60 °C. As a consequence, a distillation of FA from FA/DMSO would result in a significant decomposition of the synthesized FA, if the catalyst is still present in the mixture. Currently, all systems, which use DMSO as a solvent for FA synthesis, do not include a catalyst removal from the product mixture.[15c]

We propose here a biphasic system DMSO/*n*-heptane for the hydrogenation of $CO_2$ to FA. This approach allows facile catalyst recycling and the generation of a catalyst-free DMSO-FA product phase, which is essential for an effective isolation (Figure 3).
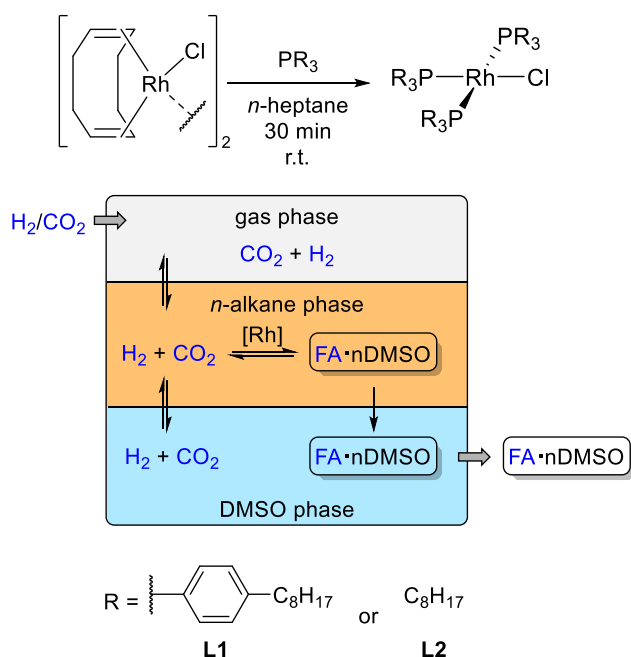


**Figure 3.** Formation of the Wilkinson-Type pre-catalyst (upper part) and depiction of the investigated biphasic catalytic approach (bottom).

To ensure high solubility and effective retention of the catalyst in *n*-heptane, Wilkinson-type complexes modified with apolar phosphine ligands were used. The pre-catalysts were formed *in situ* by adding an excess of either tris(4-octylphenyl)phosphine (**L1**) or trioctylphosphine (**L2**) to [Rh(COD)Cl]_2 (COD = 1,5-cyclooctadiene). The obtained catalyst, dissolved in *n*-heptane, was loaded into an autoclave containing DMSO. The autoclave was pressurized with $CO_2$ and $H_2$, stirred and heated until constant pressure was reached. After cooling to r.t. and depressurization, the FA containing DMSO phase was removed via syringe and replaced by a fresh batch of DMSO. The autoclave was then pressurized again for a further reaction using with the same catalyst phase. Rh- and P-content of each collected product phase were analyzed by ICP-MS for quantifying the catalyst leaching (Table 1).

**Table 1.** Rh-catalyzed hydrogenation of $CO_2$ to FA in *n*-heptane-DMSO: recycling experiments[a]

| | | | | | Leaching | |
|---|---|---|---|---|---|---|
| Ligand | Run | $t$ [h][c] | TON | $c_{FA}$ [mol/L] | P [%] | Rh [%] |
| **L1** | 1[b] | 3.8 | 129 | 1.29 | 0.42 | 0.11 |
| | 2 | 5.0 | 150 | 1.40 | 0.29 | 0.30 |
| | 3 | 12.7 | 117 | 1.22 | 0.31 | 0.35 |
| | | | 396[d] | 1.30[e] | 1.02[d] | 0.76[d] |
| **L2** | 1[b] | 0.3 | 129 | 1.34 | 0.87 | 0.07 |
| | 2 | 1.1 | 144 | 1.37 | 0.89 | 0.06 |
| | 3 | 1.9 | 140 | 1.32 | 0.92 | 0.17 |
| | 4 | 5.0 | 132 | 1.27 | 0.91 | 0.14 |
| | 5 | 20.3 | 131 | 1.21 | 0.77 | 0.12 |
| | | | 675[d] | 1.30[e] | 4.36[d] | 0.56[d] |

[a] Reaction conditions: $CO_2$ (40 bar), $H_2$ (80 bar), 60 °C, [Rh(COD)Cl]_2 (4.97 µmol), ligand (59.6 µmol, 6.5 eq), *n*-heptane (2.0 mL), DMSO (2.0 mL); [b] trioctylamine (59.6 µmol) was added; [c] the gas-uptake was monitored with a digital pressure gauge and as soon as constant pressure was observed, the reaction was regarded as completed; [d] total amount over all runs; [e] average over all runs.

The obtained results demonstrate that the envisaged biphasic approach is principally suited for catalyst immobilization and recycling. The catalyst based on the more basic alkylphosphine **L2** is more active than that based on the triphenylphosphine derivative **L1**. High FA concentrations between 1.22 and 1.40 mol/L were obtained in each run. In both cases, the catalyst activity declines with each run, but can be compensated by extended reaction times to adjust the equilibrium. The leaching values indicate that more than 99% of the metal is retained in the *n*-heptane phase even after five cycles. The excess of 3.5 equivalents of the corresponding phosphorus ligand may be responsible for a slightly higher phosphorus leaching (cf. table 1, entry 4 and 10). Despite the high catalyst retention, the increase of reaction time i.e. the decrease of catalyst activity indicates a significant

3

catalyst deactivation during the recycling experiments. Catalyst decomposition due to adventitious oxygen during the recycling procedure and/or ligand displacement by minor amounts of decomposition products of DMSO (e.g. $Me_2S$, vide infra) may be responsible for the observed decreased activity.

Importantly, after separation of the catalyst phase by decantation, the product mixture DMSO/FA was heated to 60 °C over a period of 21 h. No decrease of FA concentration was detectable furnishing the proof that such mixture can be processed as such in the downstream isolation step.

## Separation step: process design and solvent selection

We first focused on the FA purification from a DMSO/FA model mixture via distillation, which is the most applied separation technology in the chemical industry.[20] COSMO-RS predicts the existence of a temperature-maximum azeotrope between DMSO and FA. As no experimental data for the mixture of DMSO and FA are reported in literature, we performed vapor-liquid equilibrium measurements (fig. 4) which confirmed the existence of the predicted azeotrope (see ESI for experimental detail). This azeotrope must be overcome to purify FA for any DMSO-based process.
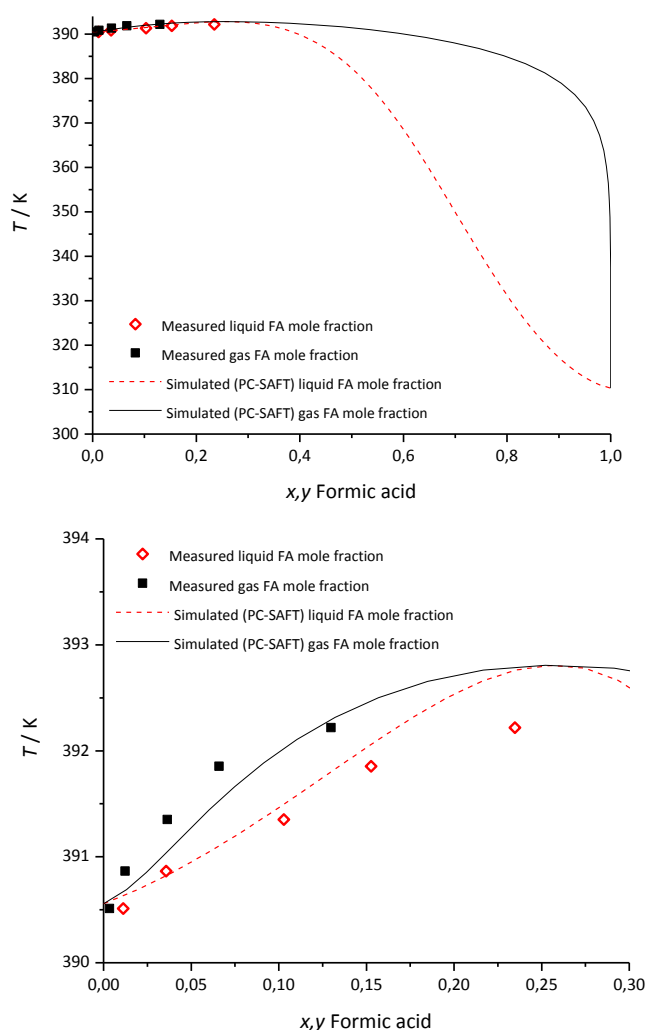




**Figure 4.** Isobaric ($p$ = 100 mbar) vapor-liquid equilibrium (VLE) for the mixture of DMSO and FA. The points show the experimental data. The continuous lines show the modeled vapor-liquid equilibrium with the equation of state PC-SAFT, where the PC-SAFT parameters have been regressed against all available experimental data. These data include the vapor-liquid equilibrium and reaction yields. Measurement and regression details can be found in the electronic supporting information (ESI). Upper figure: The diagram for the entire FA concentration range. Lower figure: Zoom for the FA mole fraction range $x/y$FA = 0−0.3.

## Entrainer strategy

Initially, we considered a traditional entrainer strategy to overcome the azeotrope.[21] As no entrainers are known for the separation of FA and DMSO, we employed phase-equilibrium data from the literature[22] to identify benzene as a suitable entrainer. Although the experimental phase-equilibrium data gives us the confidence that the separation will be feasible, multiple columns and recycles are needed in the entrainer strategy because both FA and DMSO should be recovered in pure form (process flowsheet and process details can be found in ESI). In alternative, assuming that the pressure could be further increased so that the FA yields is above the azeotrope concentration, just the amount of FA exceeding the azeotrope composition could be recovered using a single distillation column and the remaining azeotropic FA/DMSO mixture returned to the hydrogenation reactor. The use of the azeotropic DMSO-FA mixture (~24 mol. % FA) as reaction medium would inevitably lead to a lower conversion of the gaseous reactants $CO_2/H_2$. A lower conversion will in turn result in an increased need for gas recycle and related compression cost, since FA and $CO_2/H_2$ have to be separated by depressurization (fig. 2) rendering such a process highly uneconomically. Multiple recycles also complicate the operations when fluctuating $H_2$ is used as raw material. Additionally, benzene is an unfavorable entrainer due to its hazardous "nature". Therefore, the entrainer strategy was not pursued any further and an alternative approach using co-solvents was investigated for overcoming the azeotrope DMSO/FA.

## Co-solvent strategy

The use of a co-solvent should allow the recovery of all FA in pure form in a single distillation column. The co-solvent is first added to the product feed of DMSO and FA prior to the distillation (point 2 – fig. 5/6). The addition of the co-solvent dilutes the DMSO/FA feed to prevent the necessity of crossing an azeotropic point/line, thereby allowing to obtain FA in pure form at the top of the single distillation column (dashed line - fig. 6). Recovery of pure FA at the top of the distillation column (point 1 - fig. 5/6) means that DMSO diluted with co-solvent is the bottom product of the distillation (point 3 – fig. 5/6).

4

The bottom product of the distillation is recycled to the reactor to avoid further distillation columns and recycles. Therefore, in the co-solvent strategy, the FA synthesis is performed in a mixture of DMSO and co-solvent. Thus, in the co-solvent strategy, DMSO and the co-solvent fulfil distinct roles: While the presence of DMSO in the reactor sustain the FA yield, the co-solvent enables the single-column recovery of pure FA.

Obviously, the co-solvent strategy only works with suitable co-solvents. Thus, we identified 12 potential co-solvents by screening more than 5000 possible solvents with the predictive thermodynamic model COSMO-RS.[23] The screening criteria and list of co-solvents can be found in the ESI. These 12 co-solvents include carboxylic acids and aromatics such as acetic acid and 4-fluorophenol, respectively. For these co-solvents, experimental phase-equilibrium data only exist for the mixtures DMSO-acetic acid and for acetic acid-FA.[24]
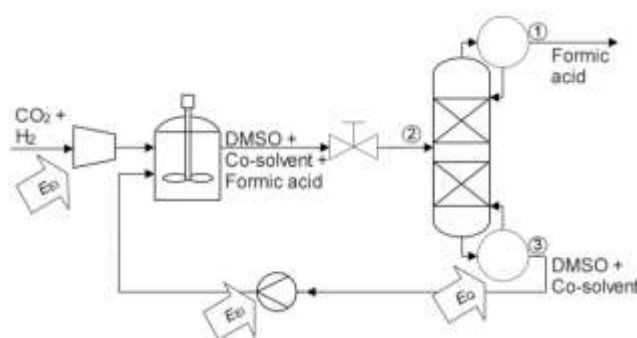


**Figure 5.** Process flowsheet of the co-solvent process strategy. Compressed $CO_2$ and $H_2$ enter the reactor together with the recycled DMSO/co-solvent mixture. After the reactor, the unreacted gases are recovered by depressurization and recycled (not shown for clarity) before FA is purified by distillation. From the bottom of the distillation column, the DMSO/co-solvent mixture is recovered and recycled. The arrows show where electricity ($E_{El}$) and heat ($E_Q$) are added to the process. The numbers 1, 2 and 3 allow to relate the positions in the distillation column to the residue-line diagram (fig. 6).

**Figure 6.** Qualitative residue-line diagram for the ternary mixture of DMSO, FA and an example co-solvent. The dashed line connects the top (Point 1), bottom (Point 3)
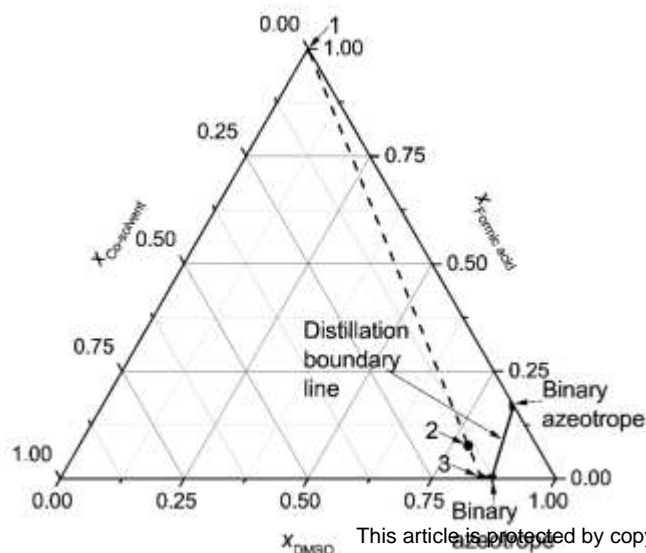


and feed (Point 2) in the distillation column (cf. fig. 5). The distillation feed (point 2) is on the side of the distillation-boundary line that allows the recovery of pure FA at the top of the distillation column (point 1).

## Energetic evaluation of the process strategies

### Objective function and assumptions

The energetic requirement for each solvent-process-strategy combination has been calculated considering both the electricity and the heating demand of the entire process. To account for these two contributions on a common basis, we measured the demand in exergy, which is the part of energy that can be turned into work.[25] Thus, exergy demand is the equivalent work demand. Furthermore, exergy has also been proposed as an assessment criterion for the environmental impact of a process.[26] The overall exergy demand ($E$) contains two contributions:

$$E = E_{EL} + E_Q$$

where the exergy demand for electricity $E_{El}$ is necessary for the pumps and compressors, and the exergy demand for heat $E_Q$ is mainly needed for the distillation (fig.°5). Exergy calculation details can be found in the ESI.

To obtain the exergy demand, we performed process simulations with Aspen Plus v.8.4 using rigorous unit-operation models. We minimized the exergy demand by optimizing the pressure in the reactor and the amount of co-solvent added to the process. The catalyst phase is not considered in the simulation due to the low mutual solubility between the phases; E.g. there is a liquid-liquid equilibrium between FA and *n*-heptane.[27]

Two accuracy levels were used in the simulations: On the first level (filled points in fig. 7), the FA yield is obtained by assuming that the reaction equilibrium is reached.[1b, 28] For this simulation level, all pure component thermodynamic data (vapor pressure, heat capacity, enthalpy of vaporization) are taken from the Aspen Plus database, which contains experimental data. The mixture thermodynamic data (activity coefficient, Henry coefficient) are taken from literature if available[24, 29] or, if not, they are calculated with COSMO-RS[30]. On the basis of these data, a first level exergy demand was predicted. On this level, 5000 co-solvents have been simulated and also the entrainer-based process for comparison. One of the lowest exergy demands was obtained for the co-solvent acetic acid (filled circle, fig.°7). Acetic acid is non-toxic, available at commercial scale and, thus, a convenient possible co-solvent. Moreover, previous studies have shown that the presence of a small portion (up to 1.33 mol/L) of AcOH and water (5 mol %) in DMSO can lead to improved catalyst performance in the hydrogenation of $CO_2$ as compared to neat DMSO.[15c]

The DMSO/acetic-acid process was then selected to be simulated on a second more accurate level

5

(open symbols in fig. 8). On this level, the modelling of the gas solubility is improved by employing the thermodynamic model PC-SAFT in the simulation of the reaction. Here, the PC-SAFT parameters that influence the hydrogen bonding in the mixture (e.g. kij) are regressed against available experimental reaction yield and vapor-liquid equilibrium data[24, 29] (including measurements from this work). To cross the distillation boundary line at a practically useful pressure of 100 mbar, a mixture is necessary with a ratio $n_{DMSO}$:$n_{AcOH}$ below 7.2 : 1. Using a $n_{DMSO}$:$n_{AcOH}$: ratio of 5 : 1 and the Ru/PTA complex reported by Moret et al. as the catalyst under standard conditions ($CO_2$: 50 bar, $H_2$: 50 bar, $T = 60$ °, $t = 120$ h), a FA concentration of 0.85 mol/L was obtained. As correctly predicted by COSMO-RS, the presence of acetic acid halves the FA concentration, i.e. from 1.90 mol/L to 0.85 mol/L (fig. 8).
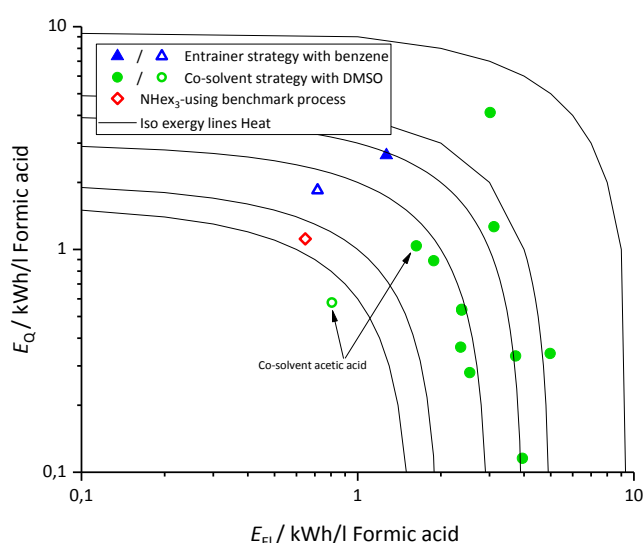


**Figure 7.** Exergy demand of identified solvent-strategy combinations and benchmarks. Each point is the exergy demand of a DMSO/co-solvent combination or benchmark in their respective strategy. The lines are iso-exergy-demand lines. The filled points show the exergy demand from the first level that employs predictions with COSMO-RS. The hollow points show the exergy demand obtained from the more accurate second level process simulations employing experimental mixture data. Calculation details can be found in the ESI.

For comparison, both the entrainer-using process and the base-using process by the BASF have been simulated on the same level of detail. All data sources and further details regarding the simulations can be found in the ESI.

*Exergetic ranking of solvent-process strategy combinations*

The lowest exergy demand was achieved by the co-solvent strategy that utilizes a mixture of DMSO and acetic acid (fig. 7). This process uses DMSO and the co-solvent acetic acid in an optimized molar ratio of $n_{DMSO} : n_{AcOH} = 7 : 1$. The DMSO/acetic-acid process

reduces the exergy demand by 45 % compared to the entrainer strategy using benzene (triangles, fig. 7).

Interestingly, the second level process simulation based on experimental mixture data results in an even lower exergy demand for the DMSO/acetic-acid process than the first level calculation. The reason for the exergy reduction is that the second level process simulation uses the experimental reaction yield which is higher than the yield predicted with COSMO-RS at the first level (fig. 7), since COSMO-RS underestimates the hydrogen-bond strength between DMSO and FA. This underestimation can be seen by comparing the measured enthalpy of mixing $H_{exp}^M = 12\ \mathbf{kJ/mol}$ [17] with the COSMO-RS predicted enthalpy of mixing $H_{exp}^M = 2.5\ \mathbf{kJ/mol}$. Therefore, a similar decrease in the exergy demand, as observed for the co-solvent acetic acid, is also likely for other co-solvents suggesting that the co-solvent strategy is promising in general. The entire list of identified co-solvents can be found in the ESI.

Noteworthy, the co-solvent strategy with DMSO/acetic acid has the lowest exergy demand $E$, not because the exergy demand for electricity $E_{El}$ or for heat $E_Q$ are, singularly taken, the lowest ones, but because the co-solvent acetic acid leads to best compromise between the exergy demands for both contributions. The exergy demand for electricity $E_{El}$ is required to increase the yield, since electricity is necessary for compressors and pumps (fig. 5) that elevate the pressure in the reactor. Similarly, the exergy demand for heat $E_Q$ is required for FA purification, since heat is added in the distillation column. Thus, the co-solvent process based on acetic acid has a low total exergy demand because acetic acid balances the trade-off between increasing the yield ($E_{El}$) and the FA purification ($E_Q$). This trade-off is reached by using the strengths of both DMSO and the co-solvent: DMSO facilitates the highest known base-free FA yield, while acetic acid allows efficient purification in a single distillation column (fig. 5/6). To avoid excessive dilution of DMSO, the amount of co-solvent is determined by the position of the binary DMSO/co-solvent azeotrope (fig. 6). Thus, the position of this binary azeotrope seems to be key with regard to the determination of the co-solvent's exergy demand. These complex relationships highlight the need for a process-level analysis to identify efficient solvents.

It has to be stressed that single column purification requires that the co-solvent acetic acid must be recycled together with DMSO to the hydrogenation reactor (fig. 5/6). In order to fulfil this requirement the catalyst system has to be compatible with AcOH in the two phase system. This prerequisite has been verified using **L2** as the ligand in n-heptane/DMSO-AcOH (again with a $n_{DMSO}$:$n_{AcOH}$ ratio of 5 : 1) under otherwise identical conditions as in Table 1. In this experiment, a FA concentration of 1.10 mol/L was obtained, a value just slightly lower than that achieved in the absence of AcOH (1.30 mol/L). The obtained FA concentration of 1.10 mol/L suggests that an even more favorable exergy balance might be

6

achieved than calculated with the conservative FA concentration of 0.85 mol/L.

Finally, we compared the DMSO/acetic acid co-solvent strategy with the BASF process.[12] This process uses the base trihexylamine (NHex$_3$) and a FA-NHex$_3$ adduct is formed upon $CO_2$ hydrogenation. Later, the FA-NHex$_3$ adduct is thermally split and two distillation columns are used for purifying FA (details in the ESI).[18] Thus, the co-solvent strategy reduces the necessary equipment and simplifies the process (cf. fig. 5), by removing one distillation column as well the catalyst extraction step carried out in a dedicated high pressure apparatus (cf. fig. 1). Moreover, the exergy demand of this NHex$_3$-using process was found by simulations to be 20 % higher than exergy demand of the co-solvent strategy with DMSO and the co-solvent acetic acid (fig. 8). However, it should be noted that there are uncertainties connected to the simulations of the NHex$_3$-using process due to missing experimental data. Nevertheless, our findings support the perception that processes based on solvent-stabilization have the potential to be energetically competitive with processes using base-stabilization for FA synthesis.
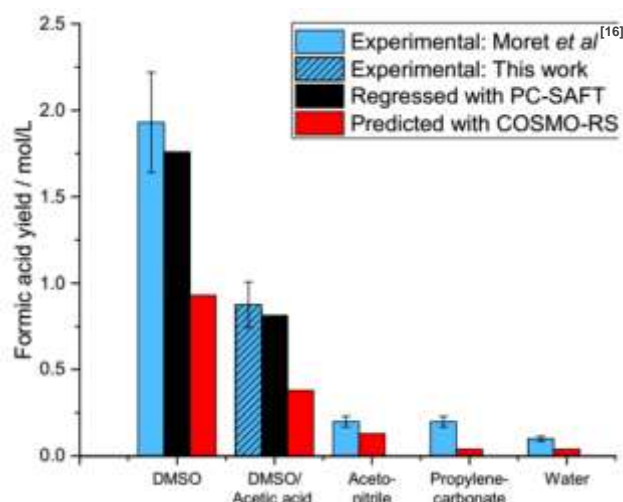


**Figure 8.** Comparison of the experimentally measured FA yield (blue), with the predictions from COSMO-RS (red) and regression with PC-SAFT (black). The error bars originate from reproducibility. The PC-SAFT parameters were regressed against both VLE data and the reaction yields.

*FA Isolation via Distillation*

To experimentally prove the isolation of FA according to the proposed co-solvent approach, we performed a batch distillation experiment with a model product phase mixture consisting of 7 mol-% FA, 76 mol-% DMSO and 16 mol-% acetic acid (cf. fig. 8). The distillation was carried out with a laboratory distillation equipment using a 250 mL round bottom flask containing 210 mL / 216 g of the model product phase mixture (7 mol-% FA, 76 mol-% DMSO and 16 mol-% AcOH). A 45 cm long filled column equipped with 0.8×0.8 mm glass rings was

used. The distillation was carried out with an oil bath temperature of 115 °C at a pressure of 100 mbar. Before the vacuum pump, a cooling trap was employed. Two fractions were collected (fraction 1: 130 mg, $T_{head}$ = 42 °C; fraction 2: 1.879 g, $T_{head}$ = 48 °C) containing a total of approx. 1.0 mol% FA from the initial 7 mol%. Both fractions contained no DMSO confirming that the predicted boundaries could be overcome and DMSO-free FA could be retrieved as top product in the distillation (cf. fig. S8). However, a variety of DMSO decomposition products were observed in all fractions and in the cooling trap. The S-containing species MeSH, Me$_2$S$_2$, 2,4-dithiapentane were identified as major components by GC-MS (ESI, fig. S9 to S14). Indeed, during the distillation, a strong sulfide smell was perceived.[31] The decomposition of DMSO has been topic of previous investigations and several pathways lead to the observed decomposition products.[32] While highly pure DMSO can be heated to its boiling point of 189 °C with only minor decomposition, small impurities can lead to an increased decomposition.[33] In the present case, the acidic conditions strongly facilitate the decomposition of DMSO (Scheme 2).
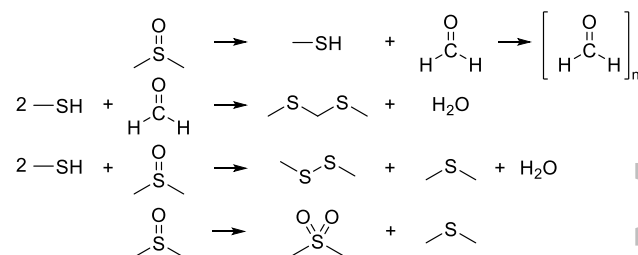


**Scheme 2.** Possible decomposition pattern of DMSO.

No decomposition products were present in the bottom liquid (cf. figure S4) probably because of the high volatility of the formed compounds. Thus, the mass balance could not be closed and no extra effort was undertaken.

## Conclusion

A process for the synthesis and isolation of formic acid from $CO_2/H_2$ was developed. The synthetic step relies on the metal-catalyzed hydrogenation of $CO_2$ in the presence of DMSO as stabilizing medium for FA. A biphasic system DMSO/*n*-heptane with tailored Wilkinson Rh-complexes was devised allowing for catalyst immobilization and metal-free product phase. Since DMSO/FA is shown to form an azeotropic mixture, simple distillation is not a viable option. Both an entrainer and a co-solvent strategy were considered for the isolation of FA via distillation. The energy demand (exergy) for the most promising systems was computed in detail. Eventually, the co-solvent strategy based on acetic acid resulted in the lowest exergy demand.

7

These results were achieved even assuming the most conservative experimental value of FA concentration of 0.85 mol/L obtained in a monophasic DMSO-AcOH mixture ($n_{AcOH}$:$n_{DMSO}$ ratio of 1:5) with a literature known catalyst. Notably, higher FA concentration of 1.10 mol/L was obtained in the hydrogenation step using the biphasic system *n*-heptane/DMSO-AcOH and **L2** as the ligand rendering the co-solvent strategy even more competitive. The distillation of a representative product mixture containing DMSO, acetic acid and FA confirmed that DMSO-free FA can be obtained. However, extensive decomposition of DMSO was observed as well. Thus, although the co-solvent process described here theoretically provides even higher efficiency compared to the state-of-the-art amine-based process, the insufficient chemical stability of DMSO during the distillation step presents a major limitation for the downstream processing. In the light of these results, alternatives to DMSO as stabilizing solvent for the hydrogenation of carbon dioxide to FA need to be identified.

## Experimental Section

**General Information:** All procedures using air-sensitive compounds were carried out under an inert argon atmosphere and application of standard *Schlenk*-technique. Unless otherwise noted, all chemicals were obtained from commercial sources and used as supplied. NMR-Spectra were recorded on an AV-400 or a DPX-300 (Bruker). Chemical shifts are reported as $\delta$ in ppm relative to tetramethylsilane ($^1$H and $^{13}$C) and 85% phosphoric acid ($^{31}$P). Hereby, the residual solvent peak of the corresponding deuterated solvents was used as internal standard for $^1$H and $^{13}$C NMR spectra. GC-MS measurements were carried out using a Variant 500-MS by Agilent with an 60m CP-WAX-52-CB Column. ICP-MS was carried out on an 8800 ICP-MS Triple Quad by Agilent with water as matrix.

**Synthesis of tris(4-octylphenyl)phosphine, L1:**[34] A 100 mL Schlenk flask equipped with a magnetic PTFE bar was loaded with magnesium turnings (240 mg, 10.0 mmol, 4.0 eq) and dried in vacuo while stirring vigorously, hereby activating the magnesium. THF (8 mL) was added. 1-Bromo-4-octylbenzene (2.16 g, 8.00 mmol, 1.90 mL, 3.2 eq) was added dropwise and the reaction mixture was stirred for 1.5 h at room temperature. During this time, the colorless suspension underwent a color change to dark green. At 0 °C phosphorous trichloride (0.343 g, 2.50 mmol, 0.220 mL, 1.0 eq) was added slowly. The reaction mixture was stirred overnight at r.t. while the dark green suspension turned yellow. The mixture was quenched with a saturated degassed aqueous ammonium chloride solution (10 mL). After extracting with n-pentane (5 × 5 mL) the reaction mixture was purified via filter column loaded with aluminum oxide and silica. After removing the solvent in vacuo the product **L1** was obtained as pale yellow oil (1.33 g, 2.23 mmol, 89%). $^1$H-NMR (300 MHz, CDCl$_3$, 25°C): $\delta$ = 7.26 - 7.17 (m, 2H, Ar-*H*), 7.16 - 7.09 (m, 2H, Ar-*H*), 2.50 (t, $^3J_{HH}$ = 8.0 Hz, 2H, C*H*$_2$), 1.70 - 1.49 (m, 2H, C*H*$_2$), 1.37 - 1.17 (m, 10H, C*H*$_2$), 0.87 (t, $^3J_{HH}$ = 6.6 Hz, 3H, C*H*$_3$) ppm. $^{13}$C-NMR (100 MHz, CDCl$_3$, 25°C): $\delta$ = 143.5 (s, Ar-*C*$_q$), 134.4 (d, $^1J_{CP}$ = 9.2 Hz, Ar-*C*$_q$), 133.7 (d, $^2J_{CP}$ = 19.5 Hz, Ar-*C*H), 128.6 (d, $^3J_{CP}$ = 7.1 Hz, Ar-*C*H), 31.9 (s, *C*H$_2$), 31.4 (s, *C*H$_2$), 29.5 (s, *C*H$_2$), 29.4 (s, *C*H$_2$), 29.3 (s, *C*H$_2$), 22.7 (s, *C*H$_2$), 14.2 (s, *C*H$_3$) ppm. $^{31}$P-NMR (160 MHz, CDCl$_3$, 25°C): $\delta$ = −7.8 (s, *P*$_{Ar}$) ppm.

**Catalytic Hydrogenation of CO$_2$ in DMSO/*n*-heptane:** In a *Schlenk*-tube, a catalyst stock solution was prepared by suspending [Rh(COD)Cl]$_2$ (49.7 µmol) in n-heptane (10 mL) and adding **L1** or **L2** (6.5 equivalents). The mixture was stirred for 15 to 30 min at room temperature. In a typical experiment, the catalyst stock solution (2 mL) was transferred into a 10 mL window autoclave and DMSO (2 mL) was added (in the first experiment of a recycling series NOct$_3$ (59.6 µmol) was added). The autoclave was pressurized at r.t. under stirring with CO$_2$ (40 bar) and H$_2$ (80 bar) to a total pressure of 120 bar. The autoclave was placed on a heating plate (60 °C) and stirred. The pressure was monitored with a digital pressure gauge. When no more pressure decrease was observed, the autoclave was cooled to r.t. and the pressure was released to approx. 1-2 bar overpressure. The remaining overpressure was released under the use of *Schlenk*-technique. The product containing DMSO phase was withdrawn via syringe and weighed. 1,4-Dioxane or mesitylene was added as a reference and a sample of the product phase was analyzed by $^1$H-NMR spectroscopy. A fresh batch of DMSO was loaded into the autoclave and pressurized described as above. This procedure was repeated until a significant decrease of catalyst activity was observed *i.e.* until the pressure decrease was significantly slower.

## Acknowledgements

## References

[1]   a) W. Reutemann, H. Kieczka, in *Ullmann's Encyclopedia of Industrial Chemistry*, 3. ed., Wiley-VCH, Weinheim, **2016**, pp. 1-22; b) J. Klankermayer, S. Wesselbaum, K. Beydoun, W. Leitner, *Angew. Chem. Int. Edit.* **2016**, *55*, 7296–7343.

[2]   a) M. Aresta, A. Dibenedetto, A. Angelini, *Chemical Reviews* **2013**, *114*, 1709-1742; b) M.

8

Pérez-Fortes, J. C. Schöneberger, A. Boulamanti, G. Harrison, E. Tzimas, *Int. J. Hydrogen Energy* **2016**, *41*, 16444-16462.

[3] a) A. Sternberg, C. M. Jens, A. Bardow, *Green Chem.* **2017**, *19*, 2244-2259; b) J. Artz, T. E. Muller, K. Thenert, J. Kleinekorte, R. Meys, A. Sternberg, A. Bardow, W. Leitner, *Chem. Rev.* **2018**, *118*, 434-504.

[4] N. von der Assen, L. J. Müller, A. Steingrube, P. Voll, A. Bardow, *Environmental Science & Technology* **2016**, *50*, 1093-1101.

[5] a) W. Leitner, *Angew. Chem. Int. Ed.* **1995**, *34*, 2207-2221; b)Y. Himeda, *European Journal of Inorganic Chemistry* **2007**, *2007*, 3927-3941; c) K. Müller, K. Brooks, T. Autrey, *Energy & Fuels* **2017**, *31*, 12603-12611.

[6] a) K. Sordakis, A. Tsurusaki, M. Iguchi, H. Kawanami, Y. Himeda, G. Laurenczy, *Green Chem.* **2017**, *19*, 2371-2378; b) J. Eppinger, K.-W. Huang, *ACS Energy Letters* **2016**, *2*, 188-195.

[7] X. W. Yu, P. G. Pickup, *J. Power Sources* **2008**, *182*, 124-132.

[8] K. Sordakis, C. Tang, L. K. Vogt, H. Junge, P. J. Dyson, M. Beller, G. Laurenczy, *Chem. Rev.* **2018**, *118*, 372-433.

[9] C. M. Jens, K. Nowakowski, J. Scheffczyk, K. Leonhard, A. Bardow, *Green Chem.* **2016**, *18*, 5621-5629.

[10] a)Y. Himeda, *Green Chem.* **2009**, *11*, 2018-2022; b) A. Boddien, F. Gärtner, D. Mellmann, P. Sponholz, H. Junge, G. Laurenczy, M. Beller, *CHIMIA International Journal for Chemistry* **2011**, *65*, 214-218; c) A. Sternberg, A. Bardow, *Energy Environ. Sci.* **2015**, *8*, 389-400; dP. Losch, A.-S. Felten, P. Pale, *Advanced Synthesis & Catalysis* **2015**, *357*, 2931-2938.

[11] W. Supronowicz, I. A. Ignatyev, G. Lolli, A. Wolf, L. Zhao, L. Mleczko, *Green Chem* **2015**, *17*, 2904-2911.

[12] T. Schaub, R. A. Paciello, *Angew. Chem. Int. Edit.* **2011**, *50*, 7278-7282.

[13] a) J. Kothandaraman, A. Goeppert, M. Czaun, G. A. Olah, G. K. S. Prakash, *Green Chem.* **2016**, *18*, 5831-5838; b) M. Scott, B. Blas Molinos, C. Westhues, G. Franciò, W. Leitner, *ChemSusChem* **2017**, *10*, 1085-1093.

[14] S. M. Lu, Z. J. Wang, J. Li, J. L. Xiao, C. Li, *Green Chem.* **2016**, *18*, 4553-4558.

[15] a) E. Graf, W. Leitner, *Journal of the Chemical Society, Chemical Communications* **1992**, 623-624; b) W. Leitner, E. Dinjus, F. Gassner, *J. Organomet. Chem.* **1994**, *475*, 257-266; c) K. Rohmann, J. Kothe, M. W. Haenel, U. Englert, M. Hölscher, W. Leitner, *Angew. Chem. Int. Ed.* **2016**, *55*, 8966-8969; d) N. V. Kolesnichenko, N. N. Ezhova, E. V. Kremleva, E. V. Slivinskii, *Russian Chemical Bulletin* **2004**, *53*, 2542-2545.

[16] S. Moret, P. J. Dyson, G. Laurenczy, *Nat Commun* **2014**, *5*, 4017.

[17] C. Fink, S. Katsyuba, G. Laurenczy, *PCCP* **2016**, *18*, 10764-10773.

[18] T. Schaub, D. M. Fries, R. Paciello, K. D. Mohl, M. Schäfer, S. Rittinger, D. Schneider, *United States Patent* **2014**, *US*, 8791297.

[19] a) T. C. Johnson, D. J. Morris, M. Wills, *Chem. Soc. Rev.* **2010**, *39*, 81-88; b) M. Grasemann, G. Laurenczy, *Energy Environ. Sci.* **2012**, *5*, 8171-8181.

[20] Ö. Yildirim, A. A. Kiss, E. Y. Kenig, *Sep. Purif. Technol.* **2011**, *80*, 403-417.

[21] J. Stichlmair, *Chem. Ing. Tech.* **1988**, *60*, 747-754.

[22] a) L. Negadi, D. a. A.-K. Vellut, A., J. Jose, *ELDATA: The International Electronic Journal of Physico-Chemical Data* **1998**, *4*, 173-178; b) R. Parashar, M. A. Ali, S. K. Mehta, *J. Chem. Thermodyn.* **2000**, *32*, 711-716.

[23] a) A. Klamt, G. Schüürmann, *J. Chem. Soc., Perkin Trans. 2* **1993**, *0*, 799-805; b) A. Klamt, V. Jonas, T. Bürger, J. C. W. Lohrenz, *J. Phys. Chem. A* **1998**, *102*, 5074-5085.

[24] S. Miyamoto, S. Nakamura, Y. Iwai, Y. Arai, *J. Chem. Eng. Data* **2001**, *46*, 405-409.

[25] M. J. Moran, H. N. Shapiro, D. D. Boettner, M. B. Bailey, *Fundamentals of Engineering Thermodynamics*, 7. ed., John Wiley & Sons, Hoboken, **2010**.

[26] a) J. Dewulf, M. E. Bösch, B. D. Meester, G. van der Vorst, H. van Langenhove, S. Hellweg, M. A. J. Huijbregts, *Environ. Sci. Technol.* **2007**, *41*, 8477-8483; b) A. Zvolinschi, S. Kjelstrup, O. Bolland, H. J. van der Kooi, *J. Ind. Econ.* **2007**, *11*, 85-98; c) M. E. Bösch, S. Hellweg, M. A. J. Huijbregts, R. Frischknecht, *Int. J. Life Cycle Ass.* **2007**, *12*, 181-190.

[27] T. Horlenko, *United States Patent* **1973**, *US*, 3718545.

[28] J. de Vries, C. J. Elsevier, in *The Handbook of Homogeneous Hydrogenation*, 1. ed., Wiley-VCH, Weinheim, **2008**, pp. 489-511.

[29] a) J. O. Spano, C. K. Heck, P. L. Barrick, *J. Chem. Eng. Data.* **1968**, *13*, 168-171; b) A. Jónasson, O. Persson, P. Rasmussen, G. S. Soave, *Fluid Phase Equilib* **1998**, *152*, 67-94; c) C. Hung Yu, J. Rong Feng, L. Ming Jer, L. Ho Mu, *J. Supercrit. Fluid.* **2008**, *44*, 273-278; d) Y. Peng, L. Ping, S. Lu, J. Mao, *Fluid Phase Equilib* **2009**, *275*, 27-32.

[30] a) C. M. Jens, K. Nowakowski, J. Scheffzcyk, K. Leonhard, A. Bardow, *Green Chem* **2016**, *18*, 5621-5629; b) J. Scheffczyk, C. Redepenning, C. M. Jens, B. Winter, K. Leonhard, W. Marquardt, A. Bardow, *Chem. Eng. Res. Des.* **2016**, *115*, 433-442.

[31] These types of compounds are commonly used as olfactory leak indicators for gas pipe and can be perceived by the human nose at very low concentrations.

[32] a) W. J. Kenney, J. A. Walsh, D. A. Davenport, *J. Am. Chem. Soc.* **1961**, *83*, 4019-4022; b) V. J. Traynelis, W. L. Hergenrother, *J. Org. Chem.* **1964**, *29*, 221-222; c) D. L. Head, C. G. McCarty, *Tetrahedron Letters* **1973**, *14*, 1405-1408; d) B. T. Brandes, D. K. Smith, *Process Saf. Prog.* **2016**, *35*, 374-391.

9

[33] Y. Babasaki, Y. Iizuka, A. Miyake, *Journal of Thermal Analysis and Calorimetry* **2015**, *121*, 295-301.

[34] S. Franks, F. R. Hartley, *J. Chem. Soc., Perkin Trans. 1* **1980**, 2233-2237.

Accepted Manuscript

## FULL PAPER

Catalytic Hydrogenation of $CO_2$ to Formic Acid: Solved and Unsolved Challenges for Process Development

*Adv. Synth. Catal.* **Year**, *Volume*, Page – Page

Christian M. Jens,[a#] Martin Scott,[b#] Bastian Liebergesell,[a] Christian G. Westhues,[b] Pascal Schäfer,[a] Giancarlo Franciò,[b] Kai Leonhard,[a] Walter Leitner[b,c]* and André Bardow[a]*